Competitive Threshold Collision-Induced Dissociation: Gas-Phase Acidity and O−H Bond Dissociation Enthalpy of Phenol

Laurence A. Angel and Kent M. Ervin*

Department of Chemistry and Chemical Physics Program, University of Nevada, Reno, Reno, Nevada 89557

Received: June 12, 2004; In Final Form: July 9, 2004

Energy-resolved competitive collision-induced dissociation methods are used to measure the gas-phase acidity of phenol relative to hydrogen cyanide. The competitive dissociation of the $[C_6H_5O{\cdot}H{\cdot}CN]^-$ complex into $C_6H_5OH + CN^-$ and $C_6H_5O^- + HCN$ is studied using a guided ion beam tandem mass spectrometer. The reaction cross sections and product branching fractions are measured as a function of collision energy. The enthalpy difference between the two reaction channels is found by modeling the reaction cross sections near threshold using RRKM theory to account for the energy-dependent product branching ratio and kinetic shift. From the enthalpy difference, the phenol gas-phase acidity, $\Delta_{acid}H_0(C_6H_5OH) = 1448 \pm 8$ kJ/mol, is determined relative to the established literature value of hydrogen cyanide, $\Delta_{acid}H_0(HCN) = 1462.3 \pm 0.9$ kJ/mol. We then derive $\Delta_{acid}H_{298}(C_6H_5OH) = 1454 \pm 8$ kJ/mol and the bond dissociation energy of $D_{298}(C_6H_5O-H) = 359 \pm 8$ kJ/mol.

1. Introduction

The O−H bond dissociation enthalpy of phenol, C_6H_5OH, is relatively small and it is the essential property in the decomposition of phenol to the phenoxy radical, $C_6H_5O^{\bullet}$. The phenoxy radical is an important intermediate in the oxidation of aromatics during combustion, but the abundance of phenoxy radical in benzene flames is significantly overpredicted by current combustion kinetics models.[1,2] An accurate enthalpy of formation of phenoxy radical, or equivalently the O−H bond dissociation enthalpy of phenol, is thus needed for modeling combustion and other kinetic processes involving these species. Despite a considerable number of gas-phase experimental measurements[3−18] and reviews[19−24] providing O−H bond dissociation enthalpy values there remains significant discrepancy in the literature. For example, a 1998 evaluation[22] by Borges dos Santos and Martinho Simões listed gas-phase $D_{298}(C_6H_5O-H)$ values ranging between 349 and 375 kJ/mol. They recommended a value of $D_{298}(C_6H_5O-H) = 371.3 \pm 2.3$ kJ/mol, based on the average value of seven selected gas-phase measurements in the range 366−375 kJ/mol. A recent compilation by Luo[24] recommends $D_{298}(C_6H_5O-H) = 368.2 \pm 6.3$ kJ/mol from a 1996 evaluation of neutral kinetics data by Tsang.[21] However, two recent guided ion beam experiments found $D_{298}(C_6H_5O-H) = 377 \pm 13$ kJ/mol and $D_{298}(C_6H_5O-H) = 381 \pm 4$ kJ/mol from the threshold energies of two proton-transfer reactions, $Cl^- + C_6H_5OH$ from our laboratory[17] and $C_6H_5OH^+ + NH_3$ from the Anderson group,[18] respectively.

We therefore believe there remains significant uncertainty in the $D_{298}(C_6H_5O-H)$ value and have returned to this system with the more recently developed energy-resolved competitive threshold collision-induced dissociation[25−27] (TCID) method. Recently, our group reported TCID measurements on proton-bound complexes of a series of alcohols using guided ion beam mass spectrometry techniques.[27,28] The results from the TCID method were in excellent agreement with previously established literature values and provided absolute acidities within ±4 kJ/mol.

2. Experimental Methods

2.1. Threshold Collision-Induced Dissociation (TCID). The competitive TCID method enables a direct measurement of the relative gas-phase acidity between an unknown and a dissimilar reference acid. For the present study, a thermalized proton-bound $[C_6H_5O{\cdot}H{\cdot}CN]^-$ anionic complex is formed. This complex is then collisionally excited at a controlled translational energy, and it dissociates into two product channels as shown in reaction 1 and Figure 1.

$$[C_6H_5O{\cdots}H{\cdots}CN]^- + Xe \rightarrow C_6H_5O^- + HCN + Xe \quad \Delta_rH_0\ (1) \qquad (1)$$

$$\rightarrow C_6H_5OH + CN^- + Xe \quad \Delta_rH_0\ (2)$$

The energy threshold difference between the two reaction channels in reaction 1 is related to the gas-phase acidities of phenol and hydrogen cyanide by eq 2.

$$\Delta E_0 = E_0(2) - E_0(1) = \delta\Delta_{acid}H_0 \qquad (2a)$$

$$\delta\Delta_{acid}H_0 = \Delta_rH_0(2) - \Delta_rH_0(1) = \Delta_{acid}H_0(HCN) - \Delta_{acid}H_0(C_6H_5OH) \qquad (2b)$$

The equality on the right-hand side of eq 2a holds if there are no reverse activation barriers for the two dissociation channels. To extract the two threshold energies, the energy-dependent branching ratio between the two channels is modeled explicitly using RRKM theory.[25−27] The acidity of phenol thus can be measured directly relative to the well-defined reference acid of HCN, for which thermochemical data are listed in Table 1.[29,30]

* Corresponding author. Electronic mail: ervin@chem.unr.edu.

10.1021/jp0474529 CCC: $27.50
Published on Web 09/11/2004

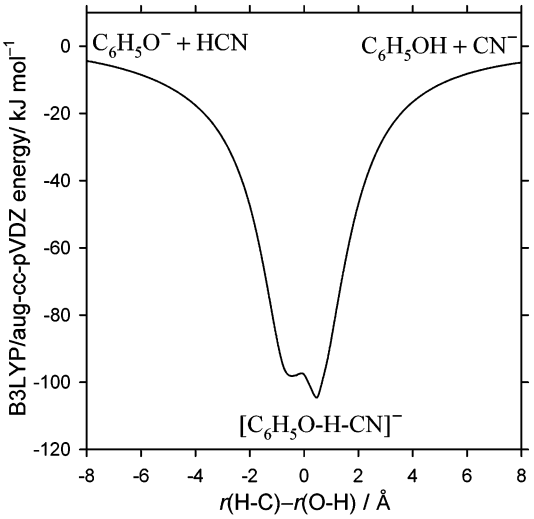

Figure 1. Potential energy surface for the dissociation of the $[C_6H_5O{\cdot}H{\cdot}CN]^-$ anionic complex in C_s symmetry. The energy relative to $CN^- + C_6H_5OH$ is plotted vs the $r(H-C) - r(O-H)$ distance at the B3LYP/aug-cc-pVDZ level of theory without ZPE corrections. See text for details.

TABLE 1: Literature Thermochemical Values

thermochemical property	value, kJ/mol	ref
$EA_0(CN)$	372.6 ± 0.4	29
$D_0(H-CN)$	522.9 ± 0.8	30
$IE_0(H)$	1312.049 ± 0.001	33
$\Delta_{acid}H_0(HCN)$	1462.3 ± 0.9	*a*
$\Delta_f H_{298}(C_6H_5OH)$	-96.4 ± 0.9	58
$\Delta_f H_{298}(H)$	217.998 ± 0.006	33
$EA_0(C_6H_5O)$	217.38 ± 0.58	15

[a] $\Delta_{acid}H_0(HCN) = D(R-H) - EA(CN) + IE(H)$.

To derive the bond dissociation energy, $D_0(C_6H_5O-H)$, we use the negative ion thermochemical cycle,[31,32] as shown below.

$C_6H_5OH \rightarrow C_6H_5O^- + H^+$	$\Delta_{acid}H_0(C_6H_5OH)$
$C_6H_5O^- \rightarrow C_6H_5O + e^-$	$EA_0(C_6H_5O)$
$H^+ + e^- \rightarrow H$	$-IE_0(H)$
$C_6H_5OH \rightarrow C_6H_5O + H$	$D_0(C_6H_5O-H)$

$$D_0(C_6H_5O-H) = \Delta_{acid}H_0(C_6H_5OH) + EA_0(C_6H_5O) - IE_0(H) \quad (3)$$

The ionization energy (IE) of the hydrogen atom is known precisely,[33] and an accurate value for the electron affinity (EA) of the phenoxy radical has been obtained by negative ion photoelectron spectroscopy,[15] as shown in Table 1.

2.2. Cross Section Measurements. Experiments were carried out using our guided ion beam tandem mass spectrometer, which has been previously described in detail.[34,35] The $[C_6H_5O{\cdot}H{\cdot}CN]^-$ complexes are formed in a flow tube reactor by producing CN^- anions in a microwave discharge from acetonitrile and adding phenol downstream of the microwave discharge. The complexes are thermalized in the flow tube by about 2×10^5 collisions with the helium buffer gas. A magnetic sector mass spectrometer is used to select the complexes before they are injected into an octopole ion beam guide where they collide with xenon atoms at a controlled translational energy. Reactant and product ions are extracted from the octopole region, mass analyzed with a quadrupole mass filter, and counted using a collision dynode/channeltron multiplier operated in negative-ion counting mode.

Absolute reaction cross sections are determined as a function of collision energy between the reactants; a thorough discussion has been presented previously.[34,36] The origin of the laboratory ion energy is measured before and after each scan by retarding potential analysis, and checked daily by a time-of-flight measurement.[34] The laboratory ion energy is then converted to the relative collision energy, E, in the center-of-mass frame.[36] To obtain absolute reaction cross sections under single collision conditions, the data are collected at three different pressures and the cross sections are extrapolated to zero pressure. The absolute cross section magnitudes have an estimated uncertainty of $\pm 50\%$, but for two product channels, the relative values are within $\pm 10\%$.

2.3. Cross Section Modeling. The single-collision reaction cross sections for both product channels, $\sigma_j(E)$, are modeled using statistical rate theory to obtain the energy difference between the two channels. Specifically, the rate constant for unimolecular dissociation of the complex to channel j is given by RRKM theory,[37,38] eq 4

$$k_j(E^*,J;E_0(j)) = \frac{s_j N^{\ddagger}_{vr,j}(E^* - E^{\ddagger}_{R,j}(J) - E_0(j))}{h\rho_{vr}(E^* - E_R(J))} \quad (4)$$

where E^* is the total internal energy of the energized molecule, $N^{\ddagger}_{vr,j}$ is the sum of active rovibrational states at the transition state configuration, ρ_{vr} is the density of states of the energized molecule, h is Planck's constant, and s_j is the reaction degeneracy. J is the angular momentum quantum number and $E_R(J)$ and $E^{\ddagger}_{R,j}(J)$ are the rotational energies of the energized molecule and transition state configuration, respectively, of the two-dimensional overall rotational motion assumed to be inactive in promoting dissociation. The transition states may be treated as fixed (tight) or orbiting (loose, i.e., located at the centrifugal barrier).[37,38] The ro-vibrational density of states is calculated using the Beyer−Swinehart Stein−Rabinovitch direct count algorithm.[39−41] The probability of dissociation of the energized complex and detection of product channel j is given by first-order reaction kinetics with parallel product channels as described by eq 5,

$$P_{D,j}(E^*,J) = \frac{k_j(E^*,J)}{k_{tot}(E^*,J)}[1 - \exp(-k_{tot}(E^*,J)\cdot\tau)] \quad (5)$$

where $k_{tot} = \sum k_j$ is the total dissociation rate constant and τ is the time-of-flight of the center-of-mass of the system from the collision cell to the mass spectrometer detector. The estimated time window varies with collision energy, but is $\tau = 9 \times 10^{-4}$ s for $[C_6H_5O{\cdot}H{\cdot}CN]^- + Xe$ near the thresholds for reaction 1. Equation 5 accounts for kinetic and competitive shifts.[42] The total internal energy of the complex E^* is given by its initial thermal energy from the ion source plus the energy ϵ transferred upon collision, using the empirical distribution function in eq 6[43]

$$P_\epsilon(\epsilon,E) = \sigma_0 N \frac{(E-\epsilon)^{N-1}}{E} \quad (6)$$

where E is the relative collision energy in the center-of-mass frame, σ_0 is a scaling factor related to the total collision cross section, and N is an adjustable parameter that describes the efficiency of translational-to-internal energy transfer. When integrated over ϵ with only the requirement that ϵ exceed the threshold energy E_0 for dissociation to occur, eq 6 yields the usual threshold law model cross section,[44] eq 7.

$$\sigma(E) = \sigma_0 \frac{(E-E_0)^N}{E} \quad \text{if } E \geq E_0 \quad \text{or}$$
$$\sigma(E) = 0 \quad \text{if } E < E_0 \quad (7)$$

TABLE 2: Rotational Constants, Vibrational Frequencies, and Hindered Rotor Parameters

	$[C_6H_5O\cdot H\cdot CN]^-$ [a]	$C_6H_5O^-$ [a]	C_6H_5OH [b]	HCN[c]	CN^- [c]
rotation (cm^{-1})	0.136, 0.026, 0.022	0.189, 0.089, 0.061	0.191, 0.089, 0.061	1.478 [2]	1.97 [2]
vibration (cm^{-1})	46,[d] 56(0.1),[e] 147(0.7), 179(1), 213(1), 226(2), 427(8), 458(8), 525(10), 531(5), 625(10), 706(11), 759(17), 830(17), 834(17), 894(21), 963(21), 986(21), 993(20), 1036(13), 1084(18), 1117(12), 1155(12), 1175(12), 1289(29), 1321(27), 1349(27), 1445(26), 1500(26), 1532(35), 1614(35), 1639(35), 2175(84), 2254(84), 3143(130), 3152(143), 3174(98), 3182(98), 3205(117)	190(2), 430(8), 443(8), 504(5), 528(5), 612(10), 687(10), 720(11), 792(17), 819(17), 846(17), 935(21), 937(21), 968(20), 1019(14), 1063(13), 1141(18), 1156(12), 1247(12), 1332(29), 1385(27), 1466(26), 1529(26), 1542(35), 1615(35), 3098(130), 3101(130), 3141(98), 3141(98), 3158(143)	245(3), 309,[d] 403(8), 409(8), 503(5), 527(5), 619(5), 686(10), 751(11), 817(17), 823(17), 888(21), 973(21), 995(20), 999(20), 1026(13), 1072(18), 1151(12), 1169(12), 1177(12), 1262(29), 1277(27), 1343(27), 1472(26), 1501(26), 1603(35), 1610(35), 3027(130), 3049(130), 3063(143), 3070(98), 3087(98), 3656(84)	713(3), 713(3), 2096(7), 3311(52)	2100(13)

torsion[f]	V_0	I	σ	n	V_0	I	σ	n
	10.5	27.5	2	2	15.8	0.93	2	2

[a] Calculated using the B3LYP/aug-cc-pVDZ method. [b] References 71 and 72. [c] Reference 52. [d] Harmonic frequency removed and treated as a hindered rotor. [e] Anharmonicities are given in parentheses. [f] Barrier heights V_0 are relative to the lowest energy minimum (kJ/mol) calculated using the B3LYP/aug-cc-pVDZ method, I is the reduced moment of inertia (amu Å^2), σ is the symmetry of the rotor, and n is the periodicity of the potential.

To model experimental cross sections, eq 5 is integrated over (a) the Boltzmann distribution of initial internal energies of the proton-bound complex, (b) the distribution of energy collisionally transferred as specified by eq 6,[43] (c) the angular momentum distribution in a statistical approximation,[25,27] (d) the Maxwell−Boltzmann thermal velocity of the target gas,[45] and (e) a Gaussian distribution of ion beam kinetic energies with the measured full-width at half-maximum.[36,46] This analysis has been discussed in detail previously, including the E and J distributions for competitive threshold collision-induced dissociation and treatment of angular momentum effects,[25−27] and is implemented using the CRUNCH program.[47]

A loose, orbiting transition state model[25,37,38] is appropriate because the complex is held together by ion−dipole forces and hydrogen bonding, rather than a covalent bond. The long-range potential including the ion-induced dipole interaction[25] and optionally the ion−permanent dipole in a locked-dipole approximation[48] is calculated using the molecular polarizability[49] and dipole moment[50] of the neutral product. Rotational and harmonic vibrational constants for the complex and products are either taken from the literature or computed at the B3LYP/aug-cc-pVDZ level using Gaussian 98[51] and are listed in Table 2. The anharmonicity constants for HCN and CN^- were taken from Gurvich et al.[52] For the aromatic ring modes of the complex, phenol, and phenoxy anion, we used anharmonicity constants calculated for benzene.[53] The anharmonicity of the OH stretching vibration has been measured by Ishiuchi et al.[54] The anharmonicity for the stretching mode corresponding to dissociation of the $[C_6H_5O\cdot H\cdot CN]^-$ complex was estimated by the Morse oscillator model and the measured complexation energy. The anharmonicity for the CO stretch was estimated at 1% of the harmonic frequency. The torsional motions around the C−O axis are treated as hindered rotors for phenol and for the $[C_6H_5O\cdot H\cdot CN]^-$ complex, using methods presented previously.[27]

The model cross sections, after being convoluted over experimental energy distributions and including the RRKM treatment described above to account for kinetic and competitive shifts, are fit to both product channels simultaneously by nonlinear least-squares optimization to obtain $E_0(1)$ and ΔE_0 along with σ_0 and N as adjustable parameters. The statistical fitting uncertainty in the relative energy is much smaller using ΔE_0 as a parameter rather than both $E_0(1)$ and $E_0(2)$, because the product branching ratio is more sensitive to ΔE_0 than to the absolute threshold energies (i.e., $E_0(1)$ and $E_0(2)$ are correlated).

3. Potential Energy Surface

The B3LYP/aug-cc-pVDZ level of theory using Gaussian 98[51] is used to investigate the potential energy surface (PES) of reaction 1. The PES shown in Figure 1 exhibits a deep double minimum well comprising two complexes $[C_6H_5OH\cdot\cdot CN]^-$ and $[C_6H_5O\cdot\cdot HCN]^-$ separated by a low-energy barrier $[C_6H_5O\cdot\cdot H\cdot\cdot CN]^-$ and connected to the $C_6H_5O^-$ + HCN and CN^- + C_6H_5OH products. The PES connecting the two minima was constructed by scanning the r(O−H) distance in 0.05 Å increments, with all other geometry parameters optimized. For the dissociation processes, we started with the optimized structure of either the $[C_6H_5OH\cdot\cdot CN]^-$ or $[C_6H_5O\cdot\cdot HCN]^-$ complex and increased the r(H−C) or r(O−H) distance by 0.2 Å increments, respectively. Geometry optimizations were performed on all other degrees of freedom apart from the angle between the C−O and C−N bonds, which was frozen at the value in the complex to avoid rotation of the two moieties back toward each other at longer range. The resulting potential energy surface is shown in Figure 1, which plots the electronic energy against r(H−C) −r(O−H). The inclusion of zero point energy (ZPE) changes the PES from an apparent double-well potential to a single well, by lowering the energy of the transition state below that of either complex. The PES in Figure 1 is not a rigorous intrinsic reaction path, but it is sufficient to prove that neither dissociation channel possesses an energy barrier. The B3LYP/aug-cc-pVDZ energies with ZPE corrections are $E_0(1) = [C_6H_5OH\cdot\cdot CN]^- \rightarrow C_6H_5O^- + HCN = 100.2$ kJ/mol and $E_0(2) = [C_6H_5OH\cdot\cdot CN]^- \rightarrow CN^- + C_6H_5OH = 104.2$ kJ/mol, predicting $\Delta E_0 = 4.0$ kJ/mol.

Calculations were also performed to check on the possibility that CN^- could induce the tautomerization of phenol to either 2,4-cyclohexadienone or 2,5-cyclohexadienone.[55] At the B3LYP/aug-cc-pVDZ level of theory with ZPE correction, geometry optimizations of CN^- with 2,4- and 2,5-cyclohexadienone found the complexes to be 130 and 111 kJ/mol higher in ZPE-corrected energy than the $[C_6H_5OH\cdot\cdot CN]^-$ complex, respectively, i.e., above either dissociation limit for reaction 1. This large energy difference represents a significant energy barrier for the forma-

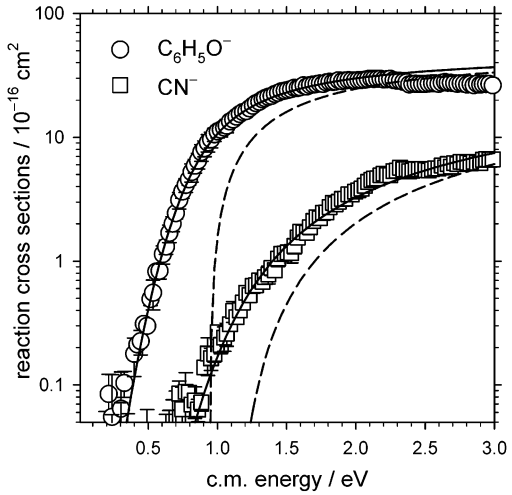

Figure 2. Single-collision TCID cross sections for $[C_6H_5O{\cdot}H{\cdot}CN]^- \rightarrow C_6H_5O^- + HCN$ (circles), $CN^- + C_6H_5OH$ (squares) as a function of relative collision energy between $[C_6H_5O{\cdot}H{\cdot}CN]^-$ and Xe. Solid lines show the convoluted fits to the data, and dashed lines show the corresponding unconvoluted 0 K model cross sections.

TABLE 3: Fitting Parameters

TS model[a]	dipole	σ_0[b]	$E_0(1)$ (eV)	ΔE_0 (eV)	N[b]
RRKM loose/loose	zero	49	0.828 ± 0.149	0.160 ± 0.035	1.3
RRKM loose/loose	locked[c]	48	0.860 ± 0.149	0.127 ± 0.035	1.3

[a] Transition state models see discussion for details. [b] σ_0 and N are fitting parameters in eqs 6 and 7. [c] The permanent dipoles of the neutral products are included in a locked dipole approximation.

tion of the cyclohexadienones in our experiment and, therefore, almost certainly excludes them. Moreover, both complexes are hydrogen bonded via nitrogen in CN^- to the cyclohexadienone. Proton transfer would initially result in HNC, which is 62 kJ/mol higher in energy than HCN.[52,56]

4. Cross Sections and Threshold Analysis

The cross sections of $C_6H_5O^- + HCN$ and $CN^- + C_6H_5OH$ products from the dissociation of the $[C_6H_5O{\cdot}H{\cdot}CN]^-$ complex are shown in Figure 2. The $CN^- + C_6H_5OH$ dissociation channel has a higher apparent threshold energy, and its cross section is about four times smaller than that of the $C_6H_5O^- +$ HCN channel. Solid lines in Figure 2 show the convoluted fits to the data while the dashed lines show the 0 K unconvoluted model cross sections (without the translational or internal energy distributions but including the RRKM branching ratio and kinetic shift). The energy range used to fit the experimental data is chosen to reproduce as much of the experimental cross section data as possible while maintaining a good fit in the threshold region. For the present work the best fits were achieved by using an energy range of 0.2−2.0 eV. It is expected that the statistical rate approximation and density of states calculations are less reliable at higher energies than near threshold. Table 3 lists the results of the empirical fits, where $E_0(1) = \Delta_c H_0$ is the dissociation threshold energy for the lower-energy channel and is equal to the complex dissociation energy of $[C_6H_5O{\cdot\cdot}HCN]^-$, and $\Delta E_0 = E_0(2) - E_0(1)$ is the energy difference between the two reaction channels.

The long-range potential for obtaining the centrifugal barrier height in the RRKM model in CRUNCH[47] has recently been modified to allow inclusion of the permanent dipole moment of the neutral products, in a locked dipole approximation.[48] As shown in Table 3, the locked-dipole method results in an increase in $E_0(1)$ by 0.032 eV and a decrease in ΔE_0 by 0.033 eV. The locked dipole method certainly over-corrects for the dipole effect, but to an unknown degree, so we use the average value of the zero dipole and locked dipole models for our reported value and expand the error bars appropriately.

TABLE 4: Thermochemical Results

property	0 K	298 K[a]
$\Delta_{acid}H(C_6H_5OH)$[b]/kJ mol^{-1}	1448 ± 8	1454 ± 8
$\Delta_{acid}S(C_6H_5OH)$[c]/J mol^{-1} K^{-1}	0	92 ± 2
$\Delta_{acid}G(C_6H_5OH)$[d]/kJ mol^{-1}	1448 ± 8	1426 ± 8
$D(C_6H_5O-H)$[e]/kJ mol^{-1}	354 ± 8	359 ± 8
$\Delta_f H(C_6H_5O)$[f]/kJ mol^{-1}	29 ± 8	44 ± 8
$\Delta_c H([C_6H_5O{\cdot\cdot}HCN]^-)$[g]/kJ mol^{-1}	81 ± 20	82 ± 20

[a] Conversion to 298 K calculated by statistical mechanics in the independent-oscillator approximation using $\Delta_r H_{298} = \Delta_r H_0 + \int_0^{298} \Delta_r C_P(T)\, dT$ with harmonic oscillator frequencies except including hindered-rotor treatments for torsions about the C−O axis. [b] Equation 2 from measured ΔE_0. [c] Gas-phase entropy calculated using the harmonic frequencies shown in Table 2 and $S_{298}(H^+)$ from Gurvich.[33] [d] $\Delta_{acid}G_{298} = \Delta_{acid}H_{298} - T\Delta_{acid}S_{298}$. [e] Equation 3. [f] $\Delta_f H(C_6H_5O) = D(C_6H_5O-H) + \Delta_f H(C_6H_5OH) - \Delta_f H(H)$. [g] From measured $E_0(1)$ threshold energy.

The error bars quoted in Table 3 are the root-sum-of-squares from individual sources of uncertainty (assuming they are independent of each other) and represent estimates of ±2 combined standard uncertainties.[57] Uncertainties were included from the ion beam energy zero determination, ±0.05 eV (lab) for $E_0(1)$, the statistical uncertainty in the least-squares fit to the data, the standard deviation from data taken on separate occasions, and the consistency of the model fit using different energy ranges. Model parameters used to fit the TCID data were also taken into consideration. The vibrational frequencies in Table 2 were varied ±20% and the experimental time window for the kinetic shift varied by a factor of 2. The final error bars for the derived thermochemical values summarized in Table 4 additionally include uncertainties from the thermochemical values used in the derivations, an estimated 0.5 kJ/mol uncertainty from the conversion from 0 to 298 K, and uncertainties derived from varying parameters used for the transition states used in the statistical rate models. The latter are described further in the discussion section.

5. Discussion

5.1. Modeling Parameters. In this section we evaluate the possible errors from choices made in the statistical rate models to fit the experimental TCID data. Estimates of these systematic uncertainties are included in the error bars listed in Table 4.

Transition State Parameters. The transition state (TS) parameters in the model were checked by comparing the loose/loose transition state combination with tight/loose, loose/tight and tight/tight combinations. The "loose" TS is the orbiting TS at the centrifugal barrier using product frequencies. The "tight" TS uses the frequencies of the $[C_6H_5O{\cdot\cdot}H{\cdot\cdot}CN]^-$ energy barrier located between the $[C_6H_5OH{\cdot\cdot}CN]^-$ and $[C_6H_5O{\cdot\cdot}HCN]^-$ complexes in Figure 1, as a limiting case. The tight/loose and loose/tight combinations resulted in very poor fits to the experimental data and therefore can be excluded. The tight/tight model, however, also provided a good fit to the data and reduced $E_0(1)$ by 0.065 eV and reduced ΔE_0 by 0.039 eV. Good fits to the data were also obtained using the tight TS for $C_6H_5O^- +$ HCN but "loosening" the tight transition state for the $C_6H_5OH + CN^-$ channel (i.e., one channel only). This loosening was done by using the frequencies of the tight transition state but reducing the four lowest vibrational frequencies by increments of 5%. Reasonable fits were obtained down to a 75%

TABLE 5: Comparison of the TCID Results with Selected Literature Values (kJ/mol)

method[a]	year	$\Delta_{acid}H_{298}(C_6H_5OH)$	$\Delta_{acid}G_{298}(C_6H_5OH)$	$\Delta_fH_{298}(C_6H_5O^{\bullet})$	$D_{298}(C_6H_5O-H)$
TCID	2004	1454 ± 8	1426 ± 8	44 ± 8	359 ± 8
MATI/GIB	2000				381 ± 4
PT/GIB	1998	≤1471 ± 13	≤1442 ± 13	≤63 ± 13	≤377 ± 13
EVAL	1998			57 ± 2	371.3 ± 2.3
EVAL	2003			54 ± 6	368.2 ± 6.3
ICR	1981	1460 ± 8	1432 ± 8		
HPMS	1978	1465 ± 8	1437 ± 8		

[a] Key: TCID, results derived from this work; MATI/GIB, proton-transfer reaction using a guided ion beam with a mass-analyzed threshold ionization source;[18] PT/GIB, proton-transfer reaction using a guided ion beam;[17] EVAL, recommended value from reviews;[22,24] ICR, equilibrium study using an ion cyclotron resonance mass spectrometer;[7] HPMS, equilibrium measurement using a high-pressure mass spectrometer.[5]

reduction. This procedure resulted in lowering $E_0(1)$ by 0.076 eV and lowering ΔE_0 by 0.002 eV. Our preferred TS model is the loose/loose combination, with the results shown in Table 3 and Figure 2. The loose/loose model is the most appropriate because the potential energy surface in Figure 1 reduces to a single well PES, after including ZPE corrections, with no barrier for either dissociation channel. On the basis of the observed variation with the other transition state treatments, we assign an additional uncertainty component of 0.04 eV for ΔE_0.

Reaction Path Degeneracy. The reaction path degeneracy, $s = \sigma/\sigma^{\ddagger}$, is the ratio of the rotational symmetry numbers of the reactant complex, σ, and the transition state, $\sigma^{\ddagger}$. For the loose/loose TS model without the hindered rotor treatment $s = 1$ for $C_6H_5OH + CN^-$ and $s = 0.5$ for $C_6H_5O^- + HCN$, but for asymmetric tight transition states, $s = 1$ for both channels. Inclusion of the hindered rotor treatment for the OH torsional motions in both the complex and phenol results in $s = 1$ for both product channels, because the rotational degeneracy is included in the density of states calculation for the rotors. Varying the reaction path degeneracies by factors of two to test these limits resulted in $E_0(1)$ varying by ±0.012 eV and ΔE_0 by ±0.03 eV.

Angular Momentum Distribution. The 2D rotational distribution of the dissociating complex is treated using a statistical estimate and explicit convolution over possible values of the rotational quantum number J, as described previously.[25,27] To check the sensitivity of our results to this model we also used either $J = 0$ or a Boltzmann rotational distribution at 300 K. These latter treatments changed $E_0(1)$ by ±0.001 eV and increased ΔE_0 by 0.009 eV for $J = 0$ and increased ΔE_0 by 0.008 eV for a rotational distribution corresponding to 300 K.

Anharmonicity. In our analysis we include vibrational anharmonicity and hindered rotors as described above. To estimate the possible error related to anharmonicity effects, we used a harmonic oscillator model, which decreased $E_0(1)$ by 0.013 eV and increased ΔE_0 by 0.004 eV. Treating the OH torsional motions as harmonic oscillators instead of as hindered rotors in the final analysis decreased $E_0(1)$ by 0.019 eV and ΔE_0 by only 0.001 eV.

The above deviations found by varying modeling parameters are treated as independent sources of uncertainty and are included in the root-sum-of-squares for the final error bars shown in Table 4, along with experimental uncertainities. (The only exception is the uncertainty derived from the dipole treatment which is treated as additive.) This treatment assumes we have at worse made randomly correct or wrong choices for the statistical model and parameters where there is a choice between models.

5.2. Thermochemical Derivations. Thermochemical values derived from the present work are summarized in Table 4. Using eq 2, we obtain $\Delta_{acid}H_0 = 1448 \pm 8$ kJ/mol. This is the primary result of this experiment; it depends on the literature acidity of HCN obtained from EA(CN)[29] and $D_0(H-CN)$[30] in Table 1, both of which appear to be reliable in our judgment. The derivation of the O−H bond dissociation enthalpy of phenol, $D_0(C_6H_5O-H) = 354 \pm 8$ kJ/mol, using eq 3 further depends on the electron affinity of phenoxy radical.[15] The photoelectron spectrum of $C_6H_5O^-$ has a well-resolved origin transition, giving a clear assignment of the electron affinity.[15] Table 4 also shows enthalpy of formation of phenoxy radical, derived from the bond energy and literature values for phenol and hydrogen atom in Table 1,[33,58] and the complexation energy of $[C_6H_5O^{\bullet\bullet}HCN]^-$, equal to $E_0(1)$ at 0 K.

We can also directly examine the cross sections shown in Figure 2 to obtain a firm upper limit for the gas-phase acidity of phenol. The cross sections show that $\Delta E_0 \geq 0.0$ eV, i.e., the CN^- cross sections rise after the $C_6H_5O^-$ cross sections. The only plausible way to have $\Delta E_0 > 0.0$ eV but $\delta\Delta_{acid}H_0 < 0$ would be for the CN^- channel to have a reverse activation barrier, but the PES in Figure 1 shows no energy barrier in either channel. Therefore, by using the well-established gas-phase acidity of $\Delta_{acid}H_0(HCN) = 1462.3 \pm 0.9$ kJ/mol as an upper limit for $\Delta_{acid}H_0(C_6H_5OH)$, we derive $D_{298}(C_6H_5O-H) \leq 373 \pm 0.9$ kJ/mol.

5.3. Comparison with Literature Experiments. The most direct comparison of our result can be made with the gas-phase acidity of phenol obtained from proton-transfer equilibrium experiments. The Gibbs energy gas-phase acidity derived from this work is $\Delta_{acid}G_{298}(C_6H_5OH) = 1426 \pm 8$ kJ/mol, in agreement within the uncertainties with the NIST recommended value of 1432 ± 8 kJ/mol from equilibrium measurements by ion cyclotron resonance (ICR) mass spectrometry.[7,59] An earlier equilibrium study by Cumming and Kebarle[5] using high-pressure mass spectrometry (HPMS) found $\Delta_{acid}G_{298}(C_6H_5OH) = 1437 \pm 8$ kJ/mol and is just within the combined uncertainties. In the equilibrium experiments, the acidity of phenol is measured relative to several acids with close-lying acidities, which are in turn anchored to the absolute acidities of HCl or HF via a long chain of interlocking equilibrium measurements. It was noted that although the agreement between the ICR and HPMS acidity scales is good overall, the agreement is poor specifically in the region of phenol.[7] The present work favors the ICR value over the HPMS value.

Table 5 compares our bond dissociation enthalpy, $D_{298}(C_6H_5O-H) = 359 \pm 8$ kJ/mol, with a selection of values reported recently in the literature. To our knowledge, the most recent independent value is the mass-analyzed threshold ionization guided ion beam experiment (MATI/GIB) by Anderson and co-workers,[18] who obtained $D_{298}(C_6H_5O-H) = 381 \pm 4$ kJ/mol from the proton-transfer reaction $C_6H_5OH^+ + ND_3$. The value is derived from a threshold fit to four points from the proton-transfer reaction which occurs in competition with a dominant H/D exchange process. Compared with our experimental value, it is outside the mutual uncertainties and it is also

TABLE 6: Comparison of Theoretical Results (kJ/mol)

method	$\Delta_{acid}H_0(C_6H_5OH)$	$EA_0(C_6H_5O)$	$D_0(C_6H_5O-H)$
G3//B3LYP	1457	225.6	366.9
CBS-QB3	1456	215.1	359.0
B3LYP/aug-cc-pVTZ	1451	213.2	345.6
expt	1448 ± 8^a	217.4 ± 0.6^b	354 ± 8^c

[a] This work. [b] Gunion et al.[15] [c] Equation 3.

higher than our qualitative upper limit of $D_{298}(C_6H_5O-H) \leq 373 \pm 0.9$ kJ/mol. The Ervin group previously used a proton-transfer reaction between $Cl^- + C_6H_5OH$ in a guided ion beam experiment (PT/GIB) to determine $D_{298}(C_6H_5O-H) = 377 \pm 13$ kJ/mol.[17] However, in a subsequent study of similar bimolecular proton transfer reactions, the threshold energies were found to systematically exceed the expected values by 5−9 kJ/mol.[60] Better results were obtained by assuming that rotational energy is not available to promote reaction. This issue of the role rotational energy in bimolecular proton-transfer reactions remains unresolved, but the value should be treated as an upper limit, $D_{298}(C_6H_5O-H) \leq 377 \pm 13$ kJ/mol.

The 1998 evaluation by Borges dos Santos and Martinho Simões[22] recommended $D_{298}(C_6H_5O-H) = 371.3 \pm 2.3$ kJ/mol, an average of seven values from gas-phase experiments that they considered to be the most reliable. The stated error bar is twice the standard deviation of the mean, while twice the population standard deviation would give 371.3 ± 5.7 kJ/mol. The present work supports a bond dissociation enthalpy that is lower than this recommendation. Given the wide range of values from the gas-phase experiments listed in the evaluation, 349 to 375 kJ/mol, it perhaps cannot be expected that the mean of the selected samples will produce the true $D_{298}(C_6H_5O-H)$ value. The value selected in the compilation by Luo,[24] $D_{298}(C_6H_5O-H) = 368.2 \pm 6.3$ kJ/mol, has overlapping error bars with the present value.

5.4. Comparison with Theory. Table 6 compares our experimental thermochemical values with selected theoretical methods[51]—G3//B3LYP,[61,62] CBS-QB3,[63,64] and B3LYP/aug-cc-pVTZ.[65−68] Calculated values for the bond dissociation energy are consistent with comparable levels of theory reported previously.[69,70] The theoretical values at various levels in Table 6 are in better agreement among themselves for the gas-phase acidity of phenol (range of 6 kJ/mol) than for the electron affinity of phenoxy radical (range of 13 kJ/mol) or the O−H bond dissociation energy of phenol (range of 21 kJ/mol). Theoretical calculation of the gas-phase acidity is more reliable than the bond energy or the electron affinity. That is because C_6H_5OH and $C_6H_5O^-$ are both closed-shell singlets with the same number of electrons, whereas the radical is an open-shell doublet. Cancellation of errors is therefore expected to be better for the acidity calculation.

The calculated acidities in Table 6 either agree with our experimental value within the error bars, or else nearly agrees in the case of G3//B3LYP. For the electron affinity, which is more precisely known experimentally,[15] the CBS-QBS and B3LYP values are in very good agreement, within 4 kJ/mol, but G3//B3LYP is in error by 8.2 kJ/mol, beyond the target accuracy of the method. That implies that the G3//B3LYP method is inadequate for this system. DeTuri and Ervin[28] reported that higher-level methods, CCSD(T)/aug-cc-pVTZ or better, are required to obtain accurate gas phase acidities within a few kilojoules per mole, on the basis of the mean absolute error for a set of (mostly smaller and nonaromatic) benchmark acids. Unfortunately, such calculations are beyond our current computational capability for phenol.

6. Conclusions

The TCID method presented here yields $D_{298}(C_6H_5O-H) = 359 \pm 8$ kJ/mol. More than half of the uncertainty arises from possible variations in transition state parameters that can be chosen for the statistical rate model. Our analysis relies on the assumptions that the collisionally activated complex dissociates statistically and that the dissociation can be modeled by RRKM theory. The present bond dissociation energy is significantly lower than recently cited $D_{298}(C_6H_5O-H)$ values in the literature (Table 5). Routine theoretical calculations of the bond dissociation energy do not converge on a single value (Table 6). Although we have confidence in our experimental and data analysis procedures, we do not anticipate that a single new measurement will resolve the discrepancies in the bond dissociation enthalpy of phenol. Future work in this laboratory will be aimed at constructing a thermochemical ladder in this region of the gas-phase acidity scale with additional reference acids. A gas-phase acidity ladder with interlocking determinations should allow the determination of an absolute $D_{298}(C_6H_5O-H)$ value from the TCID method with higher precision, as shown previously for small alcohols,[27,28] and provide an internal test of the statistical models via redundant measurements. The present work shows that although statistical modeling uncertainty contributes significantly to the uncertainty of competitive TCID with a single reference acid, when more than one transition state model can fit the data, the possible magnitude of such errors can be estimated by varying the models over reasonable ranges.

Acknowledgment. This research is supported by the U.S. Department of Energy, Office of Science, Office of Basic Energy Sciences, Chemical Sciences, Geosciences and Biosciences Division. We would like to thank Professor Peter B. Armentrout for helpful discussions and Dr. F. Ahu Akin for experimental assistance.

References and Notes

(1) Hodgson, D.; Zhang, H.-Z.; Nimlos, M. R.; McKinnon, J. T. *J. Phys. Chem. A* **2001**, *105*, 4316.
(2) Chai, Y.; Pfefferle, L. D. *Fuel* **1998**, *77*, 313.
(3) Paul, S.; Back, M. H. *Can. J. Chem.* **1975**, *53*, 3330.
(4) Colussi, A. J.; Zabel, F.; Benson, S. W. *Int. J. Chem. Kinet.* **1977**, *9*, 161.
(5) Cumming, J. B.; Kebarle, P. *Can. J. Chem.* **1978**, *56*, 1.
(6) DeFrees, D. J.; McIver, R. T., Jr.; Hehre, W. J. *J. Am. Chem. Soc.* **1980**, *102*, 3334.
(7) Fujio, M.; McIver, R. T., Jr.; Taft, R. W. *J. Am. Chem. Soc.* **1981**, *103*, 4017.
(8) Peters, K. S. *Pure Appl. Chem.* **1986**, *58*, 1263.
(9) Lin, C.-Y.; Lin, M. *J. Phys. Chem.* **1986**, *90*, 425.
(10) Arends, I.; Louw, R.; Mulder, P. *J. Phys. Chem.* **1993**, *97*, 7914.
(11) Bordwell, F. G.; Cheng, J.-P.; Harrelson, J. A., Jr. *J. Am. Chem. Soc.* **1988**, *110*, 1229.
(12) Mackie, J.; Doolan, K.; Nelson, P. *J. Phys. Chem.* **1989**, *93*, 664.
(13) Suryan, M. M.; Kafafi, S. A.; Stein, S. E. *J. Am. Chem. Soc.* **1989**, *111*, 1423.
(14) Walker, J. A.; Tsang, W. *J. Phys. Chem.* **1990**, *94*, 3324.
(15) Gunion, R. F.; Gilles, M. K.; Polak, M. L.; Lineberger, W. C. *Int. J. Mass Spectrom. Ion Processes* **1992**, *117*, 601.
(16) Hoke, S. H.; II; Yang, S. S.; Cooks, R. G. *J. Am. Chem. Soc.* **1994**, *116*, 4888.
(17) DeTuri, V. F.; Ervin, K. M. *Int. J. Mass Spectrom.* **1998**, *175*, 123.
(18) Kim, H.-T.; Green, R. J.; Qian, J.; Anderson, S. L. *J. Chem. Phys.* **2000**, *112*, 5717.
(19) McMillen, D. F.; Golden, D. M. *Annu. Rev. Phys. Chem.* **1982**, *33*, 493.
(20) Back, M. H. *J. Phys. Chem.* **1989**, *93*, 6880.
(21) Tsang, W. In *Energetics of Organic Free Radicals*; Simões, J. A., Greenberg, A., Liebman, J. F., Eds.; Blackie Academic and Professional: London, 1996; p 22.

(22) Borges dos Santos, R. M.; Martinho Simoes, J. A. *J. Phys. Chem. Ref. Data* **1998**, *27*, 707.
(23) Blanksby, S. J.; Ellison, G. B. *Acc. Chem. Res.* **2003**, *36*, 255.
(24) Luo, Y.-R. *Handbook of Bond Dissociation Energies in Organic Compounds*; CRC Press: Boca Raton, FL, 2003.
(25) Rodgers, M. T.; Ervin, K. M.; Armentrout, P. B. *J. Chem. Phys.* **1997**, *106*, 4499.
(26) Rodgers, M. T.; Armentrout, P. B. *J. Chem. Phys.* **1998**, *109*, 1787.
(27) DeTuri, V. F.; Ervin, K. M. *J. Phys. Chem. A* **1999**, *103*, 6911.
(28) DeTuri, V. F.; Ervin, K. M. *J. Phys. Chem. A* **2002**, *106*, 9947.
(29) Bradforth, S.; Kim, E.; Arnold, D.; Neumark, D. *J. Chem. Phys.* **1993**, *98*, 800.
(30) Cook, P. A.; Langford, S. R.; Ashfold, M. N. R.; Dixon, R. N. *J. Chem. Phys.* **2000**, *113*, 994.
(31) Berkowitz, J.; Ellison, G. B.; Gutman, D. *J. Phys. Chem.* **1994**, *98*, 2744.
(32) Ervin, K. M. *Chem. Rev.* **2001**, *101*, 391.
(33) Gurvich, L. V.; Veyts, I. V.; Alcock, C. B. *Thermodynamic Properties of Individual Substances*, 4th ed.; Hemisphere Publishing Corporation: New York, 1989; Vol. 1 (Elements O, H (D, T), F, Cl, Br, I, He, Ne, Ar, Kr, Xe, Rn, S, N, P and Their Compounds), Parts 1−2.
(34) DeTuri, V. F.; Hintz, P. A.; Ervin, K. M. *J. Phys. Chem. A* **1997**, *101*, 5969.
(35) Angel, L. A.; Ervin, K. M. *J. Am. Chem. Soc.* **2003**, *125*, 1014.
(36) Ervin, K. M.; Armentrout, P. B. *J. Chem. Phys.* **1985**, *83*, 166.
(37) Baer, T.; Hase, W. L. *Unimolecular Reaction Dynamics: Theory and Experiments*; Oxford University Press: New York, 1996.
(38) Gilbert, R. G.; Smith, S. C. *Theory of Unimolecular and Recombination Reactions*; Blackwell Scientific: Boston, MA, 1990.
(39) Beyer, T. S.; Swinehart, D. F. *Commun. ACM* **1973**, *16*, 379.
(40) Stein, S. E.; Rabinovitch, B. S. *J. Chem. Phys.* **1973**, *58*, 2438.
(41) Stein, S. E.; Rabinovitch, B. S. *Chem. Phys. Lett.* **1977**, *49*, 183.
(42) Chupka, W. A. *J. Chem. Phys.* **1959**, *30*, 191.
(43) Muntean, F.; Armentrout, P. B. *J. Chem. Phys.* **2001**, *115*, 1213.
(44) Armentrout, P. B. *Int. J. Mass Spectrom.* **2000**, *200*, 219.
(45) Chantry, P. J. *J. Chem. Phys.* **1971**, *55*, 2746.
(46) Lifshitz, C.; Wu, R.; Tiernan, T.; Terwilleger, D. *J. Chem. Phys.* **1978**, *68*, 247.
(47) Armentrout, P. B.; Ervin, K. M. CRUNCH, Fortran program, version 5.0 2004.
(48) Iceman, C.; Armentrout, P. *Int. J. Mass Spectrom.* **2003**, *222*, 329.
(49) Miller, T. M. Atomic and Molecular Polarizabilities. In *Handbook of Chemistry and Physics*, 83rd ed.; Lide, D. R., Ed.; CRC Press: Boca Raton, FL, 2002, p **10**-163.
(50) Lide, D. R. Dipole Moments. In *Handbook of Chemistry and Physics*, 83rd ed.; Lide, D. R., Ed.; CRC Press: Boca Raton, FL, 2002, p **9**-45.
(51) Frisch, M. J.; Trucks, G. W.; Schlegel, H. B.; Scuseria, G. E.; Robb, M. A.; Cheeseman, J. R.; Zakrzewski, V. G.; Montgomery, J. A., Jr.; Stratmann, R. E.; Burant, J. C.; Dapprich, S.; Millam, J. M.; Daniels, A. D.; Kudin, K. N.; Strain, M. C.; Farkas, O.; Tomasi, J.; Barone, V.; Cossi, M.; Cammi, R.; Mennucci, B.; Pomelli, C.; Adamo, C.; Clifford, S.; Ochterski, J.; Petersson, G. A.; Ayala, P. Y.; Cui, Q.; Morokuma, K.; Malick, D. K.; Rabuck, A. D.; Raghavachari, K.; Foresman, J. B.; Cioslowski, J.; Ortiz, J. V.; Baboul, A. G.; Stefanov, B. B.; Liu, G.; Liashenko, A.; Piskorz, P.; Komaromi, I.; Gomperts, R.; Martin, R. L.; Fox, D. J.; Keith, T.; Al-Laham, M. A.; Peng, C. Y.; Nanayakkara, A.; Gonzalez, C.; Challacombe, M.; Gill, P. M. W.; Johnson, B.; Chen, W.; Wong, M. W.; Andres, J. L.; Gonzalez, C.; Head-Gordon, M.; Replogle, E. S.; Pople, J. A. Gaussian98, Revision A.7. Gaussian, Inc.: Pittsburgh, PA, 1998.
(52) Gurvich, L. V.; Veyts, I. V.; Alcock, C. B. *Thermodynamic Properties of Individual Substances*, 4th ed.; Hemisphere: New York, 1991; Vol. 2 (Elements C, Si, Ge, Sn, Pb, and Their Compounds), Parts 1−2.
(53) Willetts, A.; Handy, N. *Chem. Phys. Lett.* **1995**, *235*, 286.
(54) Ishiuchi, S.; Shitomi, H.; Takazawa, K.; Fujii, M. *Chem. Phys. Lett.* **1998**, *283*, 243.
(55) Shiner, C.; Vorndam, P.; Kass, S. *J. Am. Chem. Soc.* **1986**, *108*, 5699.
(56) Pau, C.-F.; Hehre, W. J. *J. Phys. Chem.* **1982**, *86*, 321.
(57) Taylor, B. N.; Kuyatt, C. Guidelines for Evaluating and Expressing the Uncertainty of NIST Measurement Results. NIST Technical Note 1297; National Institute of Standards and Technology: Washington, DC, 1994.
(58) Pedley, J. B. *Thermochemical Data and Structures of Organic Compounds*; TRC Data Series; Thermodynamics Research Center: College Station, TX, 1994; Vol. 1.
(59) *NIST Chemistry WebBook*; Linstrom, P. J., Mallard, W. G., Eds.; NIST Standard Reference Database Number 69; National Institute of Standards and Technology: Gaithersburg, MD, March 2003.
(60) DeTuri, V. F.; Su, M. A.; Ervin, K. M. *J. Phys. Chem. A* **1999**, *103*, 1468.
(61) Curtiss, L. A.; Raghavachari, K.; Redfern, P. C.; Rassolov, V.; Pople, J. A. *J. Chem. Phys.* **1998**, *109*, 7764.
(62) Baboul, A. G.; Curtiss, L. A.; Redfern, P. C.; Raghavachari, K. *J. Chem. Phys.* **1999**, *110*, 7650.
(63) Jursic, B. S. *J. Mol. Struct. (THEOCHEM)* **2000**, *498*, 123.
(64) Pokon, E. K.; Liptak, M. D.; Feldgus, S.; Shields, G. C. *J. Phys. Chem. A* **2001**, *105*, 10483.
(65) Becke, A. *J. Chem. Phys.* **1993**, *98*, 5648.
(66) Dunning, T. H., Jr. *J. Chem. Phys.* **1989**, *90*, 1007.
(67) Kendall, R. A.; Dunning, T. H., Jr.; Harrison, R. J. *J. Chem. Phys.* **1992**, *96*, 6792.
(68) Woon, D. E.; Dunning, T. H., Jr. *J. Chem. Phys.* **1993**, *98*, 1358.
(69) Guedes, R.; Cabral, B.; Martinho Simoes, J.; Diogo, H. *J. Phys. Chem. A* **2000**, *104*, 6062.
(70) Couto, P.; Guedes, R.; Cabral, B.; Martinho Simoes, J. *Int. J. Quantum Chem.* **2002**, *86*, 297.
(71) Martinez, S. J.; III; Alfano, J. C.; Levy, D. H. *J. Mol. Spectrosc.* **1992**, *152*, 80.
(72) Bist, H. D.; Brand, J.; Williams, D. R. *J. Mol. Spectrosc.* **1967**, *24*, 402.